NUMERICAL SIMULATION OF ULTRASONIC DETECTION FOR CONCRETE STRUCTURE BASED ON EQUIVALENT OFFSET MIGRATION

Mingshun Hu[1,2], Juanjuan Li [3], Dongming Pan[2] and Shenen Chen[4]*

1. *China University of Mining and Technology, Key Laboratory of Gas and Fire Control for Coal Mines, Xuzhou, China; dejekdm@163.com*
2. *China University of Mining and Technology, School of Resource and Geosciences, Xuzhou, China; pdm3816@163.com*
3. *China University of Mining and Technology, IoT Perception Mine Research Center, Xuzhou, China; lijuanjuan19850110@163.com*
4. *University of North Carolina at Charlotte, Department Civil of and Environmental Engineering. Charlotte, USA; schen12@uncc.edu*

ABSTRACT

Ultrasonic wave testing is a classic Non-destructive testing (NDT) method to detect, locate and monitor the crack/fracture in construction materials. However, it is still hard to examine those small abnormal bodies since effective reflected signal from abnormity is usually rather weak. In this paper, a new ultrasound imaging technique, equivalent offset migration (EOM), is studied to demonstrate the feasibility and applicability for detecting concrete cracks. Thus, a complex numerical model along with six small scale flaws was built, and then the ultrasonic wave propagation in concrete was modeled by high order finite difference approximation method. Numerical simulation indicates that 1) there exists a strong scattering phenomenon while ultrasound propagates in concrete with multiple small scatter flaws, and 2) EOM is capable of imaging small flaws in concrete with high resolution and accuracy.

KEYWORDS

Equivalent offset migration (EOM), Common scatter point (CSP) gather, Non-destructive testing (NDT), Ultrasonic wave; Concrete

INTRODUCTION

Concrete is a composite material consisting of a binding medium with two types of particles, normally gravel and sand. Defects, such as void, crack and delamination in concrete, affect construction structures severely. Therefore, NDT technique is necessary in structural health monitoring (SHM). Currently, three important methods (sonic, ultrasonic and impact echo test), are widely used in NDT of concrete structures [1-3]. The main reason for using ultrasonic wave to assess strength of concrete is that a direct link between Young's modulus and wave velocity in an elastic media is theoretically supported. Besides, empirical relations have been long recognized between strength and modulus.

Bogas et al. (2013) evaluated the compressive strength of a wide range of structural lightweight aggregate concrete mixtures by ultrasonic pulse velocity (UPV) method [4]. Dilek (2007) discussed the application of UPV in field detection of damage to concrete in service and field quality assessment of cast-in-place concrete and masonry under construction [5]. Mohammed et al. (2011) applied both UPV and rebound hammer tests to evaluate the rubbercrete [6]. Acciani et

al. (2010) studied the ultrasonic wave propagation in concrete structures with defects based on finite element simulations [7].

As regards ultrasound data processing, frequency compounding method has been applied to the ultrasonic signals in concrete [8]. Bilgehan (2011) compared artificial neural network and adaptive neuro-fuzzy inference system used in concrete compressive strength estimation [9]. Bui and Kodjo (2013) presented that Ultrasonic travel time shift is more sensitive when used in an indirect configuration of transmission instead of in a semi-direct configuration in evaluation of concrete distributed cracks [10].

Bancroft and Geiger (2011) introduced an alternative technique initially known as common scatter point (CSP) migration and now is named equivalent offset migration (EOM) [11-15]. This method was also applied in other relative fields due to its advantage in imaging scattered waves [16, 17]. In this paper, we use numerical simulation method to determine the feasibility and effectiveness of the application of EOM in improving the accuracy and resolution of detection for flaws within concrete structure by ultrasonic wave.

SCATTERING CHARACTERISTIC OF ULTRASONIC WAVE PROPAGATION IN CONCRETE

Since concrete is a strongly heterogeneous solid including aggregates, cracks and porosity, Ultrasonic wave propagation in this material consists of a complex mixture of multiple scattering, which results in a diffusive energy transport [18].

In terms of Huygens-Fresnel principle, every point to a luminous disturbance reaches becomes a source of a spherical wave. The sum of these secondary waves determines the form of the wave at any subsequent time. Therefore, the recorded data is the sum of the disturbance. As shown in Figure 1, when the scale of flaws in concrete structure is small, the incident ultrasonic wave would be strongly diffracted and generate scattering waves. Only if the interface of the flaw is smooth and long enough, defection waves with strong energy could be generated.
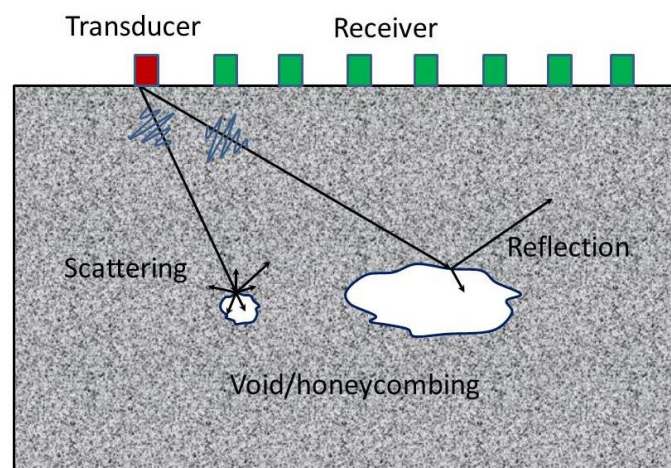

Fig. 1 - Schematic of scattered waves and reflection waves in heterogeneous concrete

In the case of the scale of the flaws being small and the concrete being highly inhomogeneous, impact echo testing method does not work. We placed transducers and sensors on the same surface which is similar to the surface geophysical exploration, and tried to apply a relatively new signal processing method in the detection of concrete structure with ultrasonic wave.

PRINCIPLE OF SCATTERED WAVE IMAGING

Double square-root (DSR) equation

Scattered wave imaging method is based on the concept of equivalent offset and CSP gather [11, 14]. We assumed that the concrete material is composed by a large number of single scatter points. Figure 2 shows the schematic of traveling path and time of scattered waves for a single scatter point. Initially, the ultrasonic waves travel from the source (transducer) to the scatter point within the concrete and then propagate backward to the receiver (sensor). Then, the receiver can record the information of the scatter point. As shown in Figure 2, MP is the middle point between the source (S) and receiver (R), and SP is the projection point of the scatter point to the observation surface. The total travel time of source-scatter point-receiver is

$$t = t_s + t_r \tag{1}$$

Where t_s is the travel time from the source to the scatter point and t_r is the travel time from the scatter point to the receiver, assuming the velocity of the acoustic wave is constant. In terms of the geometry in Figure 2, Equation 1 can be expanded as the following double square-root (DSR) equation:

$$t = \left[\frac{z_0^2 + (x+h)^2}{v^2} \right]^{\frac{1}{2}} + \left[\frac{z_0^2 + (x-h)^2}{v^2} \right]^{\frac{1}{2}} \tag{2}$$

In Equation (2), z_0 is the depth of the scatter point from the observation surface. x is the distance between MP and SP, and h is the half distance between the source (S) and receiver (R). However, the velocity of heterogeneous material is not constant. Hence, we use root-mean-square (RMS) velocity to replace the constant velocity in Equation (2) which can also be rewritten as:

$$t = \left[\left(\frac{t_0}{2} \right)^2 + \frac{(x+h)^2}{v_{rms}^2} \right]^{\frac{1}{2}} + \left[\left(\frac{t_0}{2} \right)^2 + \frac{(x-h)^2}{v_{rms}^2} \right]^{\frac{1}{2}} \tag{3}$$

Where t_0 is the vertical two-way travel time between SP and the scatter point, and v_{rms} is the RMS velocity at the position of scatter point.
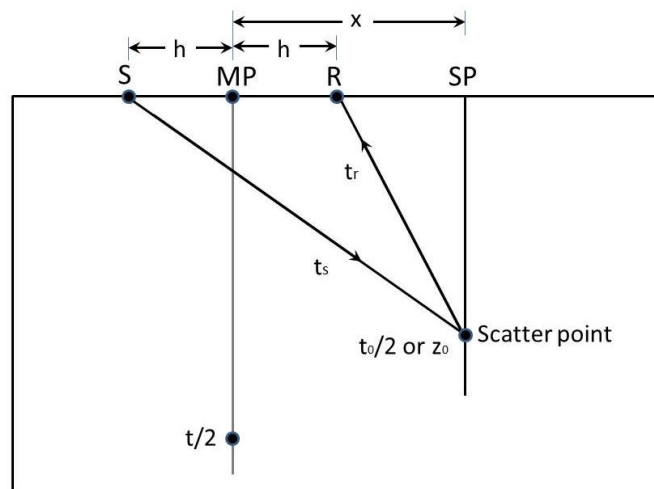

Fig. 2 - Schematic of traveling path and time of scattered waves for a single scatter point

In Figure 2, SP is the projection of scatter points to the observation surface. R is the receiver. S is the source. MP is the middle point between the source and the receiver point. t_0 is the vertical two-way travel time between point SP and scatter point. t_s is the travel time source and scatter point. t_r is the travel time between receiver and scatter point.

Equivalent offset

As shown in Figure 3, if the two-way travel time between the point E and the scatter point equals the travel time of source (S)-scatter point-receiver (R), namely $t = 2t_e = t_s + t_r$, we call the distance between point E and CSP equivalent offset. Therefore, we have the following equation:

$$t = 2t_e = 2\left[\left(\frac{t_0}{2}\right)^2 + \frac{h_e^2}{v_{rms}^2}\right]^{\frac{1}{2}} \qquad (4)$$
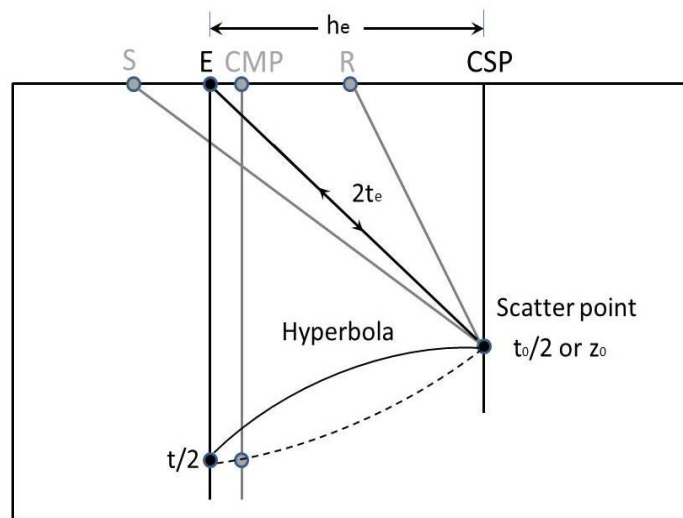

Fig. 3 - Schematic of equivalent offset

In Figure 3, CSP is the projection of scatter points to the observation surface. h_e the is equivalent offset, R is the receiver. S is the source. E is the combined equivalent source and receiver point. CMP is the middle point between source and receiver point. t_e is the travel time between point E and scatter point. t_s the is travel time source and scatter point. t_r the is travel time between the receiver and the scatter point.

Put Equation 3 into Equation 4, and then a new equation is derived as follows:

$$2\left[\left(\frac{t_0}{2}\right)^2 + \frac{h_e^2}{v_{rms}^2}\right]^{\frac{1}{2}} = \left[\left(\frac{t_0}{2}\right)^2 + \frac{(x+h)^2}{v_{rms}^2}\right]^{\frac{1}{2}} + \left[\left(\frac{t_0}{2}\right)^2 + \frac{(x-h)^2}{v_{rms}^2}\right]^{\frac{1}{2}} \qquad (5)$$

Equation 5 can be further simplified in Equation 6

$$h_e^2 = x^2 + h^2 - \left(\frac{2xh}{tv_{rms}}\right)^2 \qquad (6)$$

Therefore, we notice that under the conception of equivalent offset, the DSR Equation 2 can be transformed to single square-root Equation 6. Based on Equation 4 and 6, the common

shot gathers can be projected into the domain of common scatter point (CSP) gathers.

Fowler (1997) validated that there are several different types of hyperbolas which can be simplified from DSR Equation 2 [19]. The method based on equivalent offset is a unique way to project all data into the CSP gathers without time shift. The CSP gather, based on equivalent offset, is actually a kind of equivalent zero-offset section. Thus, the CSP gather corresponding to the point CSP on observation surface contains all information about the scatter points under the same point SP shown in Figure 3.

Equivalent offset migration (EOM)

As discussed above, in terms of Equation 4 and 6, we can project each sample in common shot gathers into CSP gathers. The CSP gathers are equivalent zero-offset sections. Therefore, as shown in Figure 4, we can integrate along the hyperbolic scattered wave events to implement the scattered wave migration based on Kirchhoff diffraction theory.
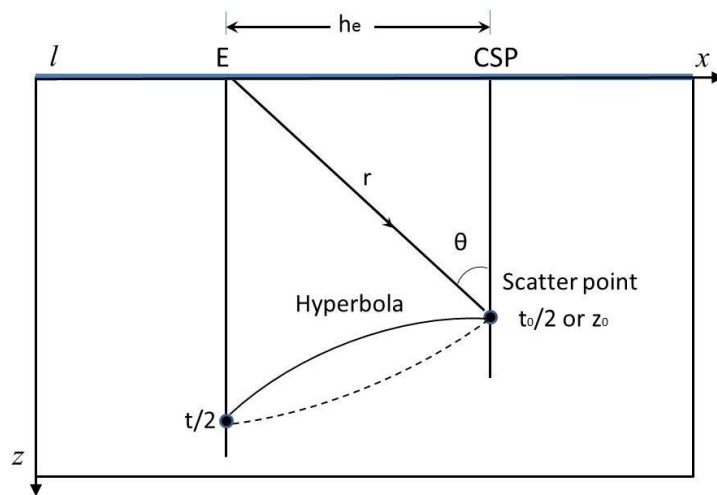

Fig.4 - Schematic of Kirchhoff integration in CSP gather

Two-dimensional Kirchhoff integration equation can be written as:

$$P(x,z;\tau) = \frac{1}{4\pi} \int_l \{\frac{1}{r}[\frac{\partial P}{\partial z}] + \frac{\cos\theta}{r^2}|P| + \frac{\cos\theta}{vr}[\frac{\partial P}{\partial t}]\}dl \qquad (7)$$

Where $P(x,y;t)$ is the acoustic wave pressure field which propagates at the velocity of $v(x,y)$, θ is the incident angle of wave, and l is the observation line, time relay $\tau = t - \frac{r}{v}$, $r = \sqrt{(h_e^2 + z_0^2)}$.

In Equation (7), the first term in the right integration is related to the gradient of pressure respect to z-direction. The second term in the right integration is called near-source term due to its attenuation by $1/r^2$. Therefore, these two terms are usually neglected in real migration due to their negligible contribution. The third term in the right integration is the basis of Kirchhoff integration migration whose discrete form is:

$$P_{out} = \frac{\Delta x}{4\pi} \sum_N \frac{\cos\theta}{vr} \frac{\partial}{\partial t} P_{in} \qquad (8)$$

Where Δx is the space between two adjacent channels in CSP gathers. $P_{out} = P(x_{out}, z; \tau = 2z_0/v)$ is the migration output wavefield based on the input wavefield $P_{in} = P(x_{in}, z = 0; \tau = t - r/v)$. Thus, we can find that this method is essentially Kirchhoff integration scatter imaging, which is called equivalent offset migration (EOM) [14].

NUMERICAL SIMULATION

To validate the effectiveness of the scattered wave imaging method, here we designed a numerical concrete model with six flaws that forms a pentagon shape shown in Figure 5. The size of this concrete model is 300 mm × 450 mm with velocity 4000 m/s. And we set the size of each flaw quite small, and all of them are 6 mm × 6 mm with velocity of 2000 m/s. The reason of this design is to determine the capability of scattered wave imaging for small scale scatter point.

In this simulation, 19 sensors are used with equal space 25 mm on the top surface of the model, and 3 sources are located in the position x = 0 mm, 200 mm and 450 mm. High order finite difference approximation is used to investigate the ultrasonic wave propagation in this kind of heterogeneous concrete. We set the cell size 2 mm and use 150 kHz Ricker wavelet as source function.
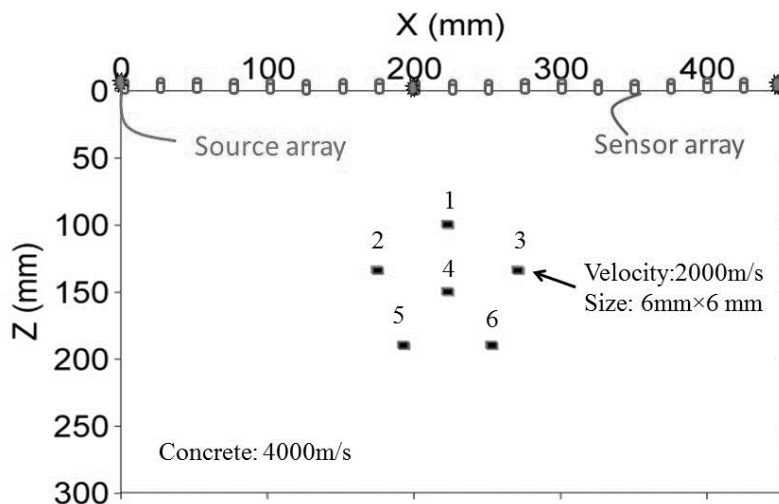

Fig. 5 - Numerical concrete model with small scale flaws

Figure 6 presents four snapshots recorded in the second shot. From these snapshots, we can notice that severe scattering waves are generated when the ultrasound hit these scatter points (flaws in small size). Each scatter point can generate new spherical wave as a new point source. All these new spherical waves later interference each other. Due to the strong scattering, the characteristic of wave field becomes quite complex. It is hard for conventional migration methods to image these small scatter points.
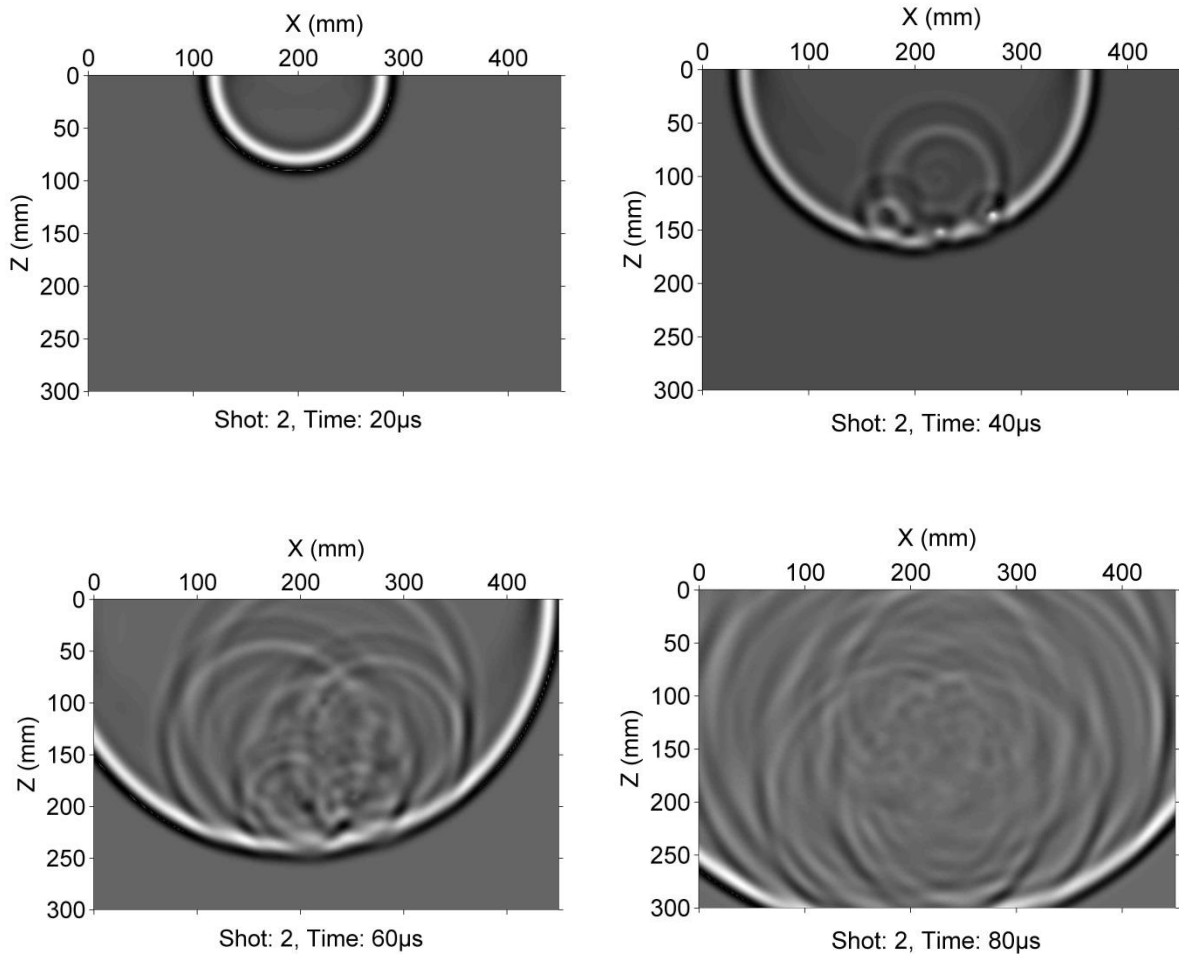
Fig.6 - Snapshot of second shot (x = 200 mm)

(a) Original records   (b) Direct wave muted records
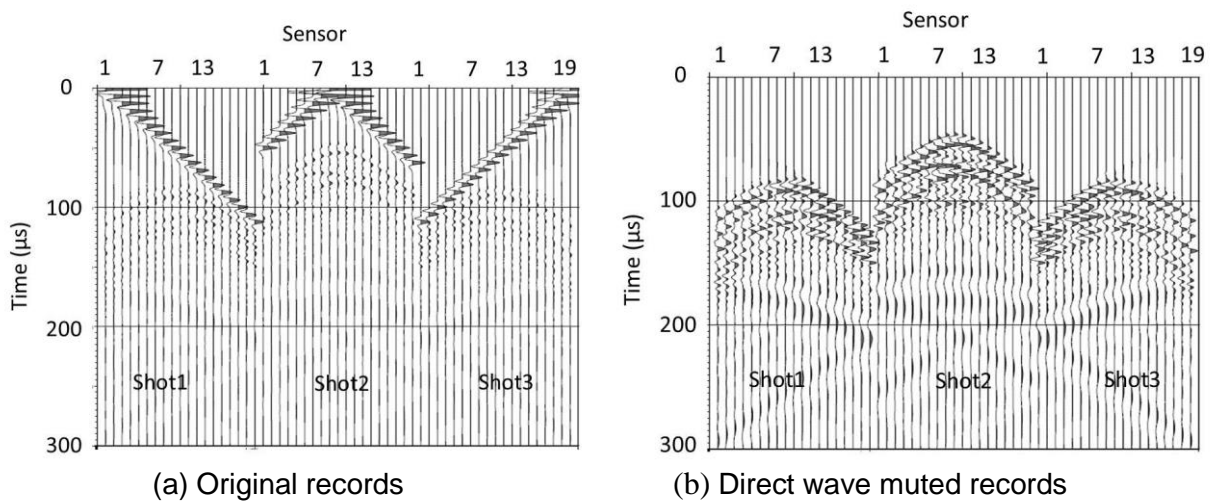
Fig.7 - Wave records

We can also find the same characteristic in wave records in Figure 7 (a) which is the original wave records. Due to the strong energy in direct waves (these waves propagate from source to receiver directly along the observation surface), the coda waves containing the

information of the inside structure of the concrete model present very low amplitude. It is not good to image the testing objects due to the interference of direct waves. Therefore, these direct waves should be muted before using scattered wave imaging. Figure 7 (b) is the wave record without direct waves.

Figure 8 is the imaging results by different migration methods. Figure 8 (a) is imaged by equivalent offset migration (EOM) and Figure 8 (b) by reverse time migration (RTM). RTM, a migration method based on wave equation, can get the best imaging result if the velocity of model is known. In other words, RTM is highly affected by the level of velocity analysis technique. However, in order to get the most accurate result and compare it with the imaging result by EOM, the imaging result in Figure 8 (b) is made by RTM with the velocity of model we created. Compared to Figure 8(b), the imaging result in Figure 8 (a) has apparent diffraction interference that is classic migration noise resulting from Kirchhoff integration migration. Additionally, the flaws, No. 5 and No. 6, are not as clear as other four flaws, especially flaw No. 1. The reason of this phenomenon is that the energy of the backward scattered waves from bottom flows is not as strong as the energy of the waves from top flows. In practice, we should improve the amplitude of the signal from the bottom structure by some energy compensation process, such as exponent gain and spherical compensation.

In addition, from the Equation (4), (6) and (8), velocity model is necessary for implementing EOM. As regards concrete detection by ultrasound, usually we can consider the velocity of ultrasound waves as a constant value. For this numerical case, the velocity we get is 3950 m/s which is a little less than the velocity of direct wave 4000 m/s. So we can see that EOM is not like RTM in the requirement of accuracy for analysis. That means EOM is quite applicable for real testing due to the difficulties in velocity analysis for real detection.
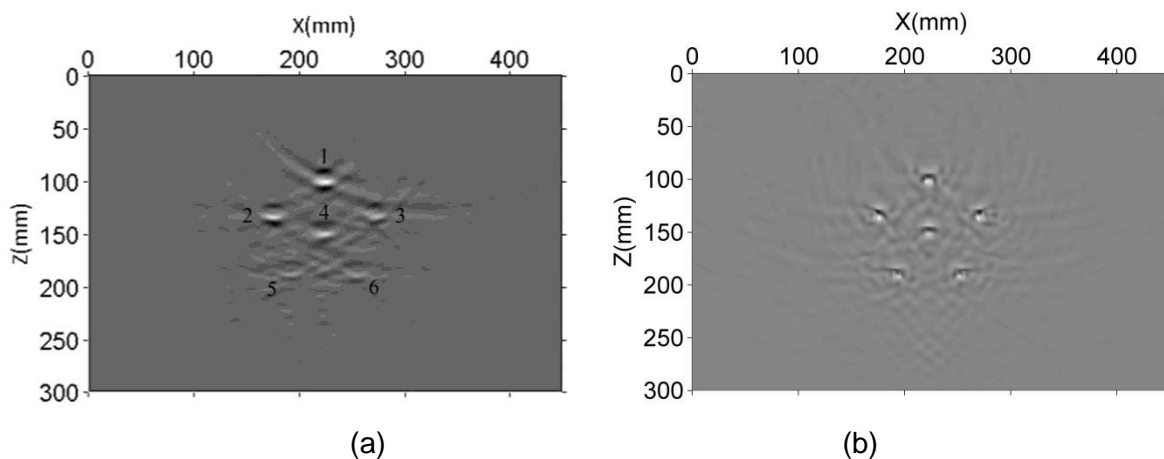

(a)   (b)

Fig. 8 - Imaging results of numerical model by EOM (a) and RTM (b)

RESULTS AND DISCUSSIONS

The above numerical simulation indicates that EOM is good at utilizing scattered waves to image very small scale structures. The main reason is that EOM is a pre-stack migration method based on the scattering wave theory. In terms of Equation (4) and (6), CSP gathers can be projected from original shot gathers under the conception of equivalent offset with the Huygens principle. CSP gathers is actually a type of equivalent zero-offset section, and we can easily apply Kirchhoff integration to image these scatter points (the whole testing object volume can be thought as the mixture composited by a large number of single scatter points). Due to the basic theory of EOM, it is suitable to apply EOM to detect the heterogeneous materials, such as concrete with different kinds of flaws and aggregates. It is also possible that EOM can be extended into other

----

fields of detection, such as metal plate damage evaluation.

CONCLUSIONS

This paper investigated the effectiveness of EOM applied in detecting concrete structures by ultrasonic waves. In terms of the conception of equivalent offset and Kirchhoff integration migration, we built a numerical concrete model, with six small scale flaws, to determine the applicability and feasibility of EOM for concrete structure detection by ultrasonic waves. The simulation result shows EOM is a great imaging method for detecting small scale concrete defects. However, some physical modelling tests should be carried out to evaluate it deeply in the future.

ACKNOWLEDGEMENTS

REFERENCES

[1]   Mccann D. M., Forde M. C., 2001. Review of NDT methods in the assessment of concrete and masonry structures. NDT & E International, 34(2): 71-84.

[2]   Aggelis D. G., et al., 2011. Longitudinal waves for evaluation of large concrete blocks after repair. NDT & E International, 44(1): 61-66.

[3]   De Belie N., et al., 2005. Ultrasound monitoring of the influence of different accelerating admixtures and cement types for shotcrete on setting and hardening behaviour. Cement and Concrete Research, 35(11): 2087-2094.

[4]   Bogas J. A., Gomes M. G., Gomes A., 2013. Compressive strength evaluation of structural lightweight concrete by non-destructive ultrasonic pulse velocity method. Ultrasonics, 53(5): 962-972.

[5]   Dilek U., 2007. Ultrasonic Pulse Velocity in Nondestructive Evaluation of Low Quality and Damaged Concrete and Masonry Construction. Journal of Performance of Constructed Facilities, 21(5): 337-344.

[6]   Mohammed B. S., Azmi N. J., Abdullahi M., 2011. Evaluation of rubbercrete based on ultrasonic pulse velocity and rebound hammer tests. Construction and Building Materials, 25(3): 1388-1397.

[7]   Acciani G., et al., 2010. Nondestructive evaluation of defects in concrete structures based on finite element simulations of ultrasonic wave propagation. Nondestructive Testing & Evaluation, 25(4): 289-315.

[8]   Ho K. S., et al., 2012. Application of frequency compounding to ultrasonic signals for the NDE of concrete. AIP Conference Proceedings, 1430(1): 1508-1515.

[9]   Bilgehan M., 2011. A comparative study for the concrete compressive strength estimation using neural network and neuro-fuzzy modelling approaches. Nondestructive Testing & Evaluation, 26(1): 35-55.

[10]   Bui D., et al., 2013. Evaluation of Concrete Distributed Cracks by Ultrasonic Travel Time Shift Under an External Mechanical Perturbation: Study of Indirect and Semi-direct Transmission Configurations. Journal of Nondestructive Evaluation, 32(1): 25-36.

[11]   Bancroft J. C., Geiger H. D., 1994. Equivalent offset CRP gathers. SEG Technical Program Expanded Abstracts 1994, 672-675.

[12]   Bancroft J. C., Xu Y., 1999. Equivalent offset migration for vertical receiver arrays. SEG Technical Program Expanded Abstracts 1999, 1279-1282.

----

[13]   Bednar J. B., 1999. A theoretical comparison of equivalent‐offset migration and dip moveout‐prestack imaging. GEOPHYSICS, 64(1): 191-196.

[14]   Bancroft J. C., Geiger H., Margrave G., 1998. The equivalent offset method of prestack time migration. GEOPHYSICS, 63(6): 2042-2053.

[15]   Khaniani H., Bancroft J. C., 2011. Enhancing the inversion of migration velocity by implementation of tilt effects on CSP data. SEG Technical Program Expanded Abstracts 2011, 3882-3886.

[16]   Hu M., Pan D., Li J., 2010. Numerical simulation scattered imaging in deep mines. Appl Geophys, 7(3): 272-282.

[17]   Zhang T. X., et al., 2009. Application of the equivalent offset migration method in acoustic log reflection imaging. Appl Geophys, 6(4): 303-310.

[18]   Schubert F., Marklein R., 2002. Numerical Computation of Ultrasonic Wave Propagation in Concrete Using the Elastodynamic Finite Integration Technique (EFIT). IEEE Ultrasonics Symposium 2002, 799-804.

[19]   Fowler P. J., 1997. A comparative overview of prestack time migration methods. SEG Technical Program Expanded Abstracts 1997, 1571-1574.